

UB  
NASA TM X-1145

FACILITY FORM 502  
 X 65 7-23-66  
 ACCESS ON REQUEST  
 31  
 JUL 25 1966  
 IN BACK OF COVER ONLY  
 (REAR)  
 2  
 23  
 (REAR)

# PREDICTING THERMAL CONDUCTIVITY OF TUNGSTEN — URANIUM DIOXIDE DISPERSIONS

*by John V. Miller*  
*Lewis Research Center*  
*Cleveland, Ohio*

CLASSIFICATION CHANGED  
UNCLASSIFIED

TO: T.O. 72-285 Date 7/17/71  
By Authority of \_\_\_\_\_

NATIONAL AERONAUTICS AND SPACE ADMINISTRATION • WASHINGTON, D. C. • SEPTEMBER 1965

NOTED

PREDICTING THERMAL CONDUCTIVITY OF TUNGSTEN -  
URANIUM DIOXIDE DISPERSIONS

By John V. Miller

Lewis Research Center  
Cleveland, Ohio

~~RESTRICTED DATA~~

~~ATOMIC ENERGY ACT OF 1954~~

~~GROUP 1~~

~~Excluded from automatic  
downgrading and declassification~~


~~CLASSIFIED DOCUMENT-TITLE UNCLASSIFIED~~

~~This material contains information affecting the  
national defense of the United States within the  
meaning of the espionage laws, Title 18, U.S.C.,  
Secs. 793 and 794, the transmission or revelation  
of which in any manner to an unauthorized person  
is prohibited by law.~~

~~NOTICE~~

~~This document should not be returned after it has  
satisfied your requirements. It may be disposed  
of in accordance with security regula-  
tions or the provisions of the Industrial  
Security Manual for Safe-Guarding Classified  
Information.~~

NATIONAL AERONAUTICS AND SPACE ADMINISTRATION



# PREDICTING THERMAL CONDUCTIVITY OF TUNGSTEN - URANIUM DIOXIDE DISPERSIONS (U)

by John V. Miller  
Lewis Research Center

## SUMMARY


One of the parameters that must be known to determine the operating temperature of fuel elements in a nuclear reactor is the thermal conductivity of the material. When the material is a dispersion (fuel particles imbedded in a matrix of a second material), the determination of the thermal conductivity without extensive experimentation is difficult because of the complex parameters involved.

Several analytical methods, which can be used to predict the conductivity in such systems, were examined and each was found to be valid over certain ranges. Unfortunately, much of the work being done on tungsten - uranium dioxide is in a region that is not specifically covered by any of the models; however, because of the similarity between two of the analytical models, a method which in essence allows extrapolation into this region is suggested. Comparison with experimental values shows that the method results in favorable predictions.

Data were then generated by this method to determine the thermal conductivity of many tungsten - uranium dioxide combinations found in nuclear reactor analyses.

## INTRODUCTION

To establish the operating temperature of the fuel elements in a nuclear reactor, it is necessary to know the neutron flux distribution, the coolant flow rate and temperature, the heat-transfer coefficient, the fuel element geometry, and the physical properties of the material that influence the temperature under both steady-state and transient conditions. Among the properties, the thermal conductivity of the material is essentially the



[REDACTED]

controlling factor in determining the difference between the fuel element surface temperature  $T_w$  and the maximum ("centerline") temperature  $T_{\max}$  existing within the material during steady-state operation. Equation (1) expresses this temperature difference for a simple, one-dimensional, flat-plate geometry in which the thermal conductivity is independent of temperature:

$$T_{\max} - T_w = \frac{QL^2}{8K} \quad (1)$$

(Symbols are defined in appendix D.)

For a constant heat-generating rate  $Q$  and plate thickness  $L$  the temperature difference is inversely proportional to the thermal conductivity of the fueled material. When a fuel element is operating near its maximum allowable temperature, based on either mechanical or metallurgical considerations, it becomes extremely important to establish the thermal conductivity of the material.

Many fuel elements are made by melting two or more metals into a composite in which the fuel material is homogeneously alloyed with the other metals. In such alloys the mechanism of heat transfer by conduction is relatively simple, and the determination of the thermal conductivity of the composite alloy can be made with the same techniques that are used for pure metals. In general, the thermal conductivity of the alloy at a given temperature is only a function (not necessarily linear) of the relative amounts of the various materials contained in the composite, and the conductance of such a system can be determined by a minimum number of experimental points.

For a dispersion fuel in which the heat-generating material consists of individual particles distributed within a matrix of a nonfuel material, the problem of determining the thermal conductivity is further complicated by the fact that the composite material may have heterogeneous properties. The mechanism of heat conduction in such a system is more complex than that of an alloy, and the size, shape, and orientation of the particles, as well as the relative amount and properties of the material involved, become important factors in the determination of the thermal conductivity of the dispersion.

While it is possible to obtain measurements of the effective thermal conductivity of dispersions by the same techniques used for alloys, extrapolation to points that are not coincidental with those determined experimentally is difficult because of the additional variables (particle size, shape, and orientation) associated with the dispersions. It becomes important, therefore, to understand more fully the exact nature of the conduction process for such a material.

The purpose of this study is to investigate analytical methods applicable to dispersion fuels and to evaluate such methods by comparison with experimental results. In particular, the behavior of tungsten - uranium dioxide dispersions (W-UO<sub>2</sub>) are of major

concern in the tungsten - water-moderated nuclear rocket reactor program (ref. 1).

## ANALYTICAL METHODS FOR PREDICTING THERMAL CONDUCTIVITY

In conjunction with the study of electric and dielectric constants, the problem of predicting the conductivity of heterogeneous materials has been treated mathematically by a variety of investigators. Much of this work has been summarized by Powers (ref. 2) and indicates that there are two or three analytical models which are directly applicable to dispersion fuels. The first of these is the Rayleigh-Maxwell dilute dispersion equation (ref. 2, p. 7):

$$K_{\text{eff}} = K_m \left[ \frac{2K_m + K_p - 2V_p(K_m - K_p)}{2K_m + K_p + V_p(K_m - K_p)} \right] \quad (2)$$

where  $K_{\text{eff}}$  is the effective conductivity of the composite.

Because of the assumptions made in the derivation of this model, equation (2) is only applicable for dilute dispersions, where the particle concentration is less than 10 to 15 volume percent (ref. 2, p. 26). A more general equation for variable dispersions derived by Bruggeman (ref. 2, p. 10) should be applicable for any concentration. (Theoretically, this statement would only apply up to a concentration of 74.05 volume percent since this is the maximum packing density for spheres stacked in a rhombohedral array.) The form of the equation for this model is given by equation (3) and was developed by first differentiating the Rayleigh-Maxwell equation (eq. (2)) and then by integrating it between the appropriate limits.

$$K_{\text{eff}} = K_p + (1 - V_p)(K_m - K_p) \left( \frac{K_{\text{eff}}}{K_m} \right)^{1/3} \quad (3)$$

Basically, there is little difference between the results obtained by using equation (2) and those obtained by using equation (3). This becomes evident when these equations are applied to a series of cases where the ratio of the conductivities of the two phases varies from 10 to 50. Figures 1(a) to (d) show the result of this study for the thermal conductivity of the matrix greater than that of the particle ( $K_m > K_p$ ) and also when the inverse was true ( $K_p > K_m$ ). Figure 2 shows the difference between the two models expressed as the ratio of the effective conductivity predicted by the dilute dispersion equation (eq. (2)) to that predicted by the variable dispersion model (eq. (3)).

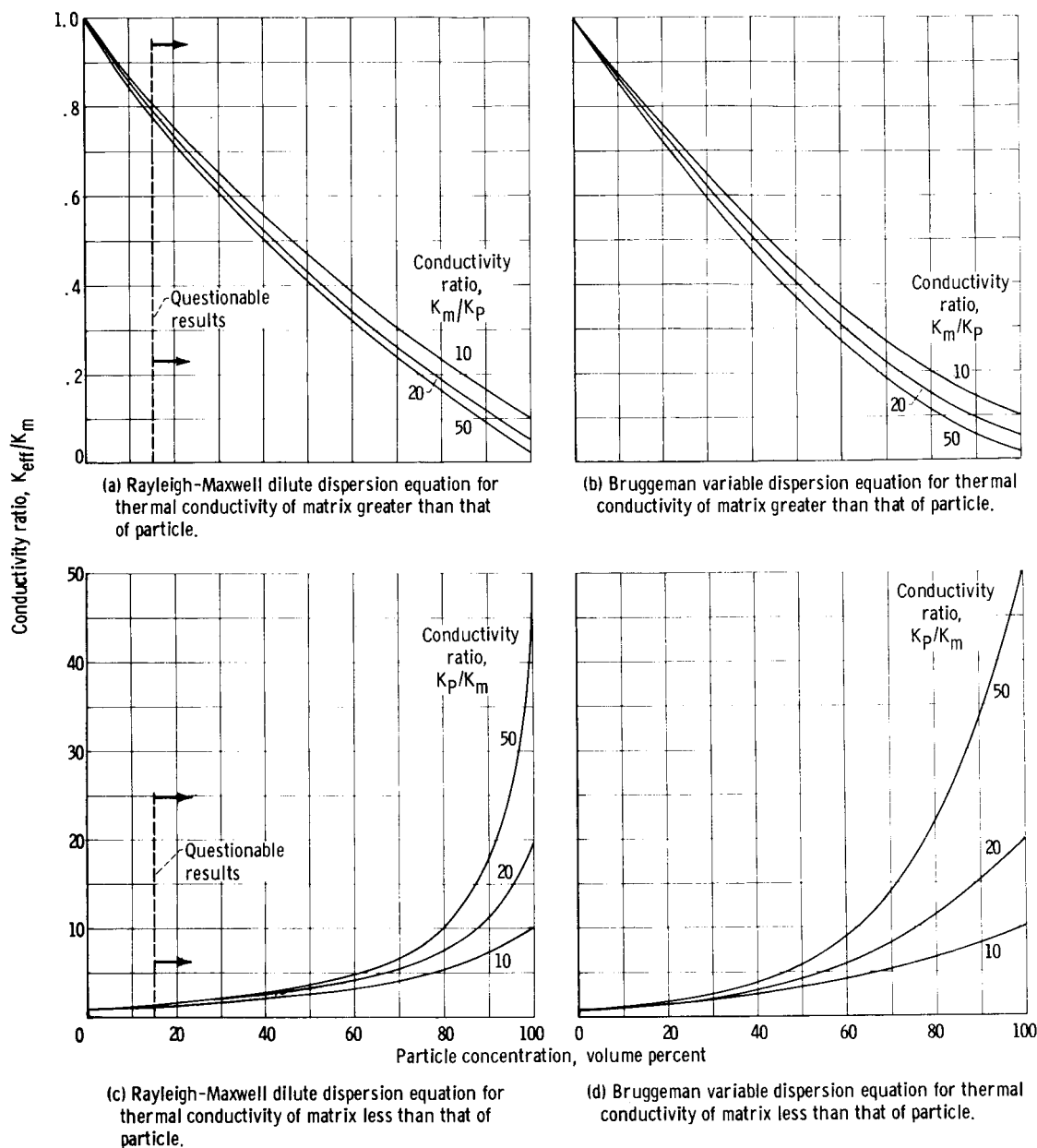


Figure 1. - Effective thermal conductivity of dispersions predicted by various models.

Although the maximum error in both cases is about the same (e.g., the maximum error is 50 to 55 percent for a conductivity ratio of 50), it should be noted that the rate of disagreement between the two models at low particle concentrations is much greater when the conductivity of the particle is higher than that of the matrix ( $K_p > K_m$ ). For example, at a conductivity ratio of 50, a 5-percent difference occurs between the two equations at a particle concentration of 36 volume percent when the conductivity of the matrix has the higher value; when the conductivity of the particle is higher, a difference

of 23 percent exists at the same concentration (36 volume percent).

Because these conditions are actually beyond the recommended limits of the dilute dispersion equation ( $>10$  to 15 volume percent), the absolute value of the error is academic and is only important in establishing the areas where similarity between the two methods would allow the use of either model with a minimum error. The use of this similarity will be discussed in the next section.

## Anisotropic Effects

The two models described in the previous section (eqs. (2) and (3)) are somewhat idealized because they are derived for materials in which the dispersed particles are spherical and the behavior is isotropic in nature. Many materials do not always behave in this ideal manner; frequently, the particles are elongated in one direction because of certain steps in the manufacturing process (e.g., rolling a material tends to elongate the particles), and the resulting properties are not isotropic as the models for spherical particles indicate.

Some work has been done on the anisotropic effects of such particles. A discussion of the various models is given in reference 2 (pp. 12 to 23), and the conclusion reached is that, for mathematical treatment, all particles can be classified as either prolate (axis  $A > B = C$ ) or oblate (axis  $A < B = C$ ) ellipsoids, or, as they are sometimes called, spheroids.

Anisotropic effects are simulated by changing the relative size and orientation of

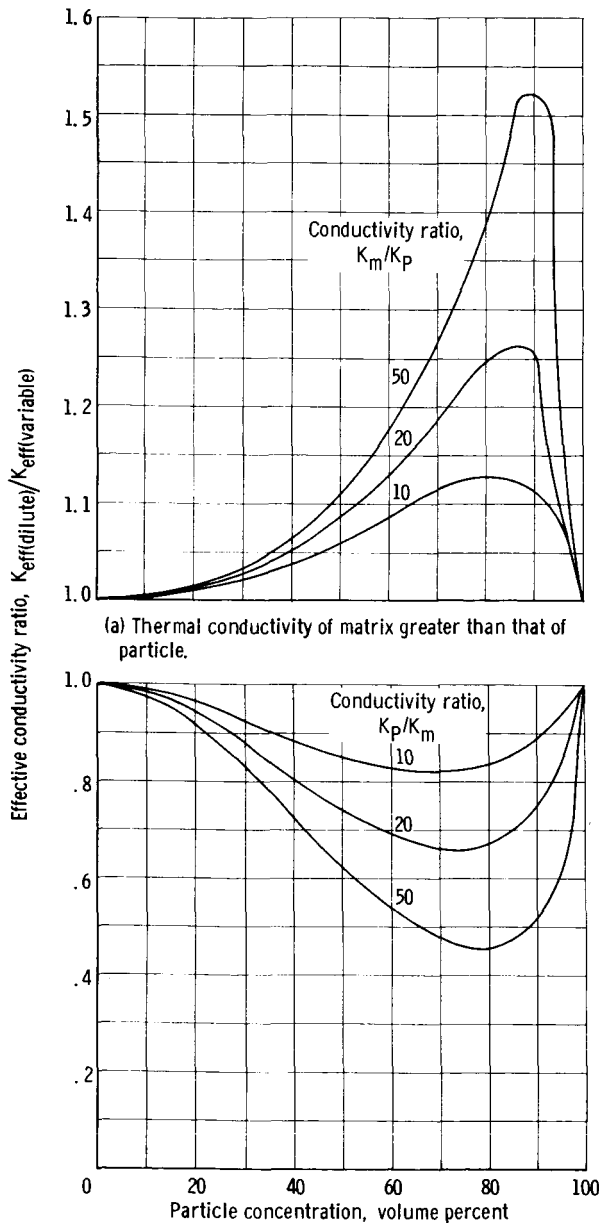
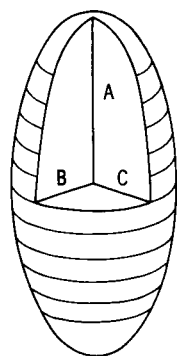
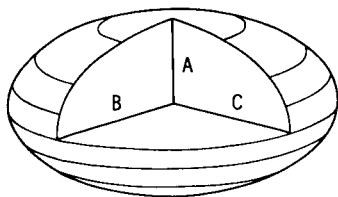


Figure 2 - Difference in effective thermal conductivity predicted by dilute and variable dispersion models.



(a) Prolate ellipsoid;  
A > B; B = C.



(b) Oblate ellipsoid; A < B; B = C.

Figure 3. - Particle shapes used in anisotropic analysis.

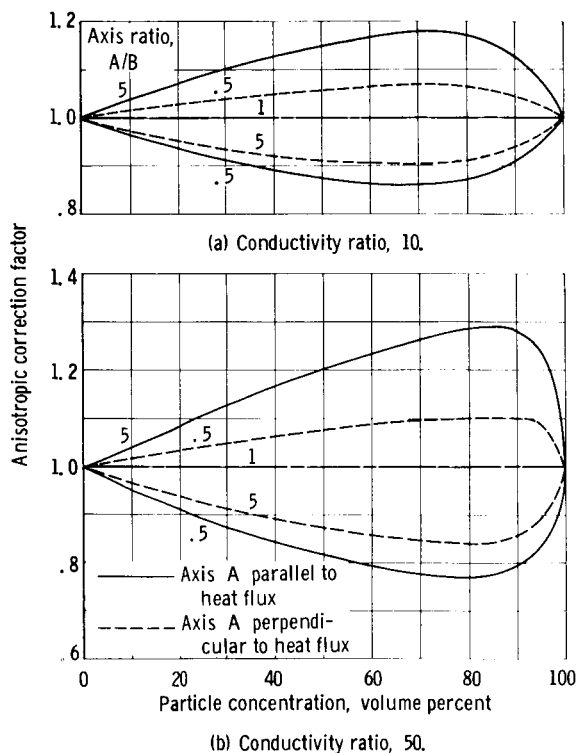


Figure 4. - Variation of anisotropic correction factor with several parameters. Conductivity of matrix greater than that of particle.

the axes of the ellipsoids with respect to the heat flux. A schematic representation of these elliptical particles is shown in figure 3.

Of the various anisotropic models described in reference 2, the one that seems most applicable to the dispersion fuel problem is the method of Fricke (ref. 2, pp. 18 to 19). The equation depicting this model can be summarized as follows:

$$K_{\text{eff}} = K_m \left[ 1 + \left( \frac{V_p \beta}{1 - V_p} \right) \left( \frac{K_{\text{eff}} - K_p}{K_m - K_p} \right) \right] \quad (4)$$

where  $\beta$  is a function of the particle shape and orientation. (The formulation of the Fricke model and the associated function  $\beta$  for various conditions is shown in appendix A.)

In the limit, as the particles become spherical in shape, this equation (eq. (4)) reduces to the Rayleigh-Maxwell dilute dispersion equation (eq. (2)). In the other extreme (i. e., as the prolate ellipsoids approach long cylinders, or the oblate ellipsoids approach thin platelets in shape), this equation reduces to the appropriate model, several of which are discussed in reference 2 (pp. 1 to 18).

Defining an anisotropic correction factor as the ratio of the effective conductivity predicted by equation (4) to that predicted by equation (2) and applying this definition to a variety of cases result in the values shown in figure 4. Again it should be noted that the dilute dispersion equation (eq. (2)) is only applicable for particle concentrations of less than 10 to 15 volume percent.

For the variable dispersion model (eq. (3)), the formulation of an anisotropic equation similar to equation (4) is not practical



because, according to Powers (ref. 2), the functions "vary with composition as well as with ellipsoidal shape and orientation and so, the mathematics would be extremely difficult." The question that arises then is how to treat those nonspherical particles for which the concentrations are greater than those values for which the dilute dispersion equations apply.

When the elongation of the particle becomes extreme, and the particle concentration is high enough that contact of adjacent particles occurs, the dispersion equation is no longer applicable. A more suitable model is a mixture equation such as the one derived by Bruggeman (ref. 2, pp. 9 to 10). This equation applies to the so-called mixtures where neither phase is completely surrounded by the other phases. The generalized equation for this model, including the anisotropic effects of particle shape and orientation, is given by

$$\left( \frac{K_m - K_{eff}}{K_m + XK_{eff}} \right) = \left( \frac{V_p}{1 - V_p} \right) \left( \frac{K_{eff} - K_p}{K_p + XK_{eff}} \right) \quad (5)$$

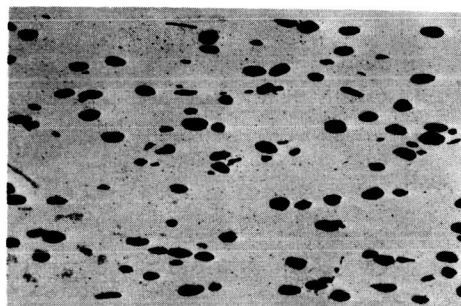
where  $X$  is defined by

$$X = \left[ \frac{K_m + K_p(\beta - 1)}{K_p - K_m(\beta + 1)} \right] \quad (6)$$

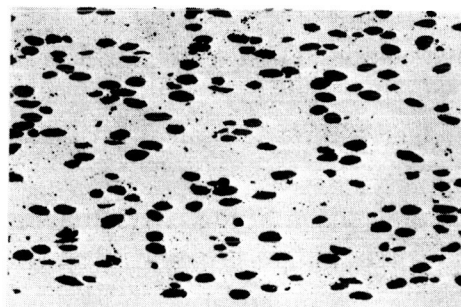
and  $\beta$  is the same function that was used in equation (4).

As the value of  $X$  varies from zero to infinity, equation (5) represents the equation for models ranging from series laminates ( $X = 0$ ) through spherical particles ( $X = 2$ ) to parallel cylinders ( $X = \infty$ ). When the particle concentration exceeds 10 to 15 volume percent, the applicability of the dilute dispersion equations (eqs. (2) and (4)) is questionable. A similar situation occurs for the mixture equation (eq. (5)) when the particles are not sufficiently elongated nor of sufficient concentration to cause interaction (contact) between particles.

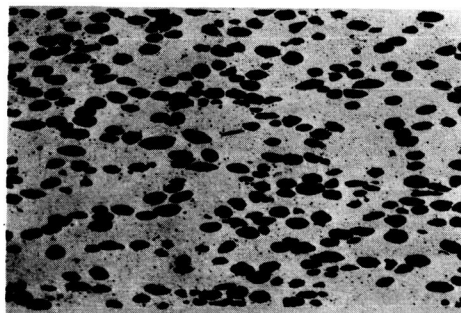
The boundaries loosely described by the above statement are not as well defined as is the concentration limit of 10 to 15 volume percent in the dilute dispersion equation because it is a function of both the elongation and the concentration. Figure 5 shows typical photomicrographs of W-UO<sub>2</sub> dispersions being considered for fuel plates in the tungsten - water-moderated nuclear rocket reactor. In general, each UO<sub>2</sub> particle is completely surrounded by the tungsten matrix; and, because the concentration is greater than the previously established limit of 10 to 15 volume percent, this material falls into the area between the dilute dispersion model (eqs. (2) and (4)) and the mixture model (eq. (5)).



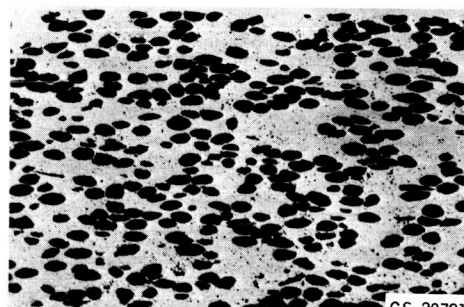
90 Tungsten - 10 uranium dioxide



80 Tungsten - 20 uranium dioxide



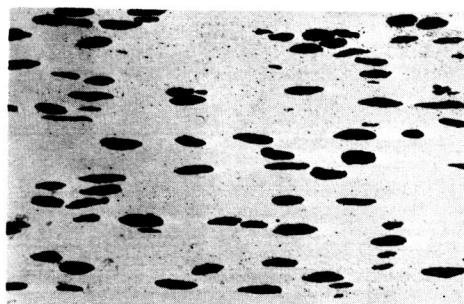
70 Tungsten - 30 uranium dioxide



60 Tungsten - 40 uranium dioxide

CS-29781

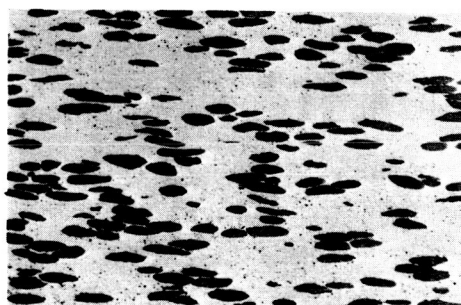
(a) Perpendicular to rolling direction.



90 Tungsten - 10 uranium dioxide



80 Tungsten - 20 uranium dioxide



70 Tungsten - 30 uranium dioxide



60 Tungsten - 40 uranium dioxide

CS-29782

(b) Parallel to rolling direction.

Figure 5. - Microstructure of tungsten - uranium dioxide plates of various fuel loadings. Composition by volume percent.

Unfortunately, in this region between the models, the mathematics for an anisotropic form of the variable dispersion equation becomes extremely difficult (ref. 2, p. 21). Careful examination of the values shown in figure 1 (p. 4) indicates that the predicted conductivity for spherical particles, when either the variable dispersion equation (eq. (3)) or the dilute dispersion equation is used, is quite similar for concentrations of less than 40 volume percent if the conductivity of the matrix is greater than that of the particles (i. e.,  $K_m/K_p > 1.0$ ).

In most cases for which the above restrictions apply, the difference between the two methods does not vary by more than 6 percent. It is conceivable, if not probable, that such a relation would also exist if an anisotropic variable dispersion equation were available to compare with equation (4).

Because the W-UO<sub>2</sub> fuel material falls into this restrictive category, that is, particles which are slightly elongated with  $K_m/K_p > 1$  and  $10 < V_p < 40$  volume percent, it is suggested that the following method be used to determine the effective thermal conductivity in this range:

(1) Calculate the effective thermal conductivity of the material by using the variable dispersion model (eq. (3)) and by assuming that the particles are spherical.

(2) Calculate an anisotropic correction factor by using the ratio of the conductivities predicted by equations (2) and (4).

(3) Determine the corrected, anisotropic conductivity of the material by multiplying the value obtained from equation (3) with the anisotropic correction factor.

This method in essence makes the assumption that the anisotropic behavior of the variable dispersion model is similar to that of the dilute dispersion model and in effect results in a thermal conductivity that can be expressed as the variable dispersion value times a shape correction factor:

$$K_{\text{eff(corrected)}} = K_{(3)} \left[ \frac{K_{(4)}}{K_{(2)}} \right] \quad (7)$$

where the numerical subscripts refer to the values obtained from equations (2), (3), and (4). Application of this method (eq. (7)) to some experimental data is shown in the section COMPARISON WITH EXPERIMENTAL RESULTS.

Because the formulation of this method (eq. (7)) is somewhat deductive rather than strictly mathematical (i. e., based on the similarity between the dilute and variable dispersion models), the use of the mixture equation (eq. (5)) to predict the anisotropic behavior of dispersions in this region might be considered. As discussed previously (p. 7), this model is not directly applicable unless the particle concentration and elongation are such that interaction between particles results. Nevertheless, to ascertain the extent

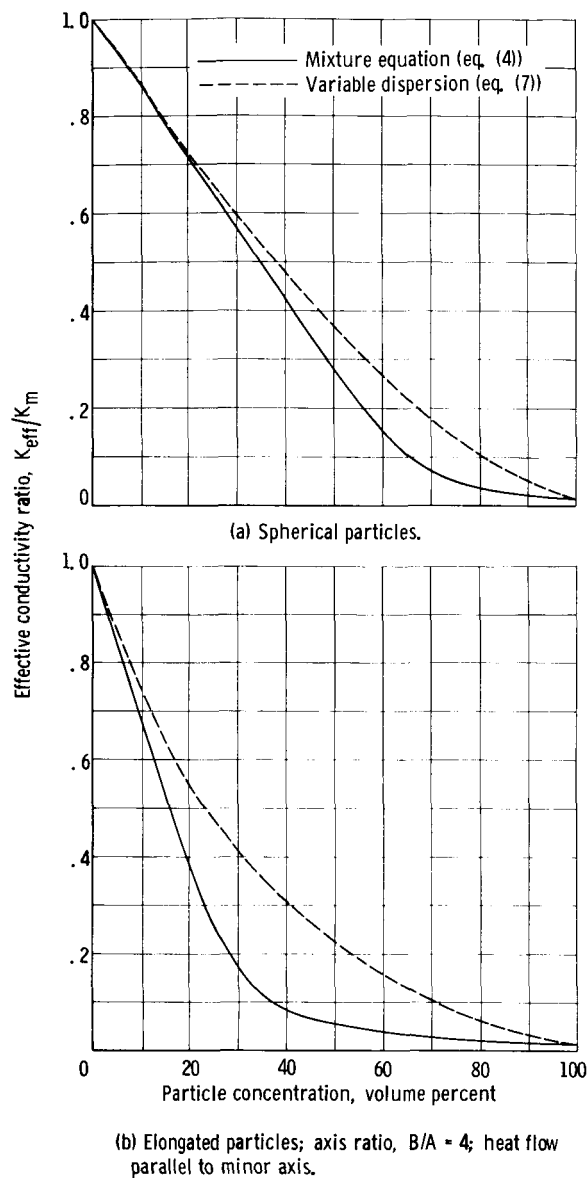


Figure 6 - Comparison of effective thermal conductivity predicted by different models; conductivity ratio, 62.

that the mixture model (eq. (5)) differs from the suggested model (eq. (7)), a typical set of calculations was performed with both methods. The results are shown in figure 6 and indicate that under isotropic conditions (spherical particles) the difference between the two methods is less than 10 percent up to particle concentrations of 40 volume percent (fig. 6(a)). When elongation of the particles occurs (fig. 6(b)), however, the difference between the two methods increases to 75 percent at the same composition (40 volume percent). If in the following sections, agreement is shown to exist between the suggested method (eq. (7)) and the experimental data, it follows that the use of the mixture model (eq. (5)) could not produce the same agreement and hence could not be used over this same range.

## Coated Particles

Frequently, the particles in the W- $UO_2$  dispersions are coated with a third material before compacting to either preserve the integrity of the individual particles or to prevent direct contact between them during fabrication. If this third material has properties different from those of either of the major constituents, the mixed or mean thermal con-

ductivity of the dispersion will be changed according to the quantity and characteristics of the coating material. Although not presently applicable to the tungsten - water-moderated reactor design, a discussion of this model will be presented herein in the event that such a material might be considered at some later date.

Kerner (ref. 2, pp. 23 to 25) derived a mathematical solution to the coating problem by considering the electric fields induced in a dispersed material by an external field. The resulting equation describing the mixed thermal conductivity of spherical particles  $p$  coated with material  $c$  and dispersed in a matrix  $m$  is given by

$$K_{\text{eff}} = \frac{K_m V_m + K_p V_p \gamma_{p,m} + K_c V_c \gamma_{c,m}}{V_m + V_p \gamma_{p,m} + V_c \gamma_{c,m}} \quad (8)$$

where the ratios of the mean field strengths are

$$\gamma_{p,m} = \frac{9K_m K_c}{(K_p + 2K_c)(K_c + 2K_p) + 2\left(\frac{V_p}{V_p + V_c}\right)(K_m - K_c)(K_c - K_p)}$$

and

$$\gamma_{c,m} = \frac{3K_m(K_p + 2K_c)}{(K_p + 2K_c)(K_c + 2K_p) + 2\left(\frac{V_p}{V_p + V_c}\right)(K_m - K_c)(K_c - K_p)}$$

and where

$$V_m + V_p + V_c = 1$$

While this model (eq. (8)) is only applicable to dispersions containing coated spherical particles, the same approach is used that was used in equation (7) to obtain a suitable correction factor that permits extrapolation to otherwise undefined regions.

In the limit, that is, as the volume of the coating  $V_c$  decreases to zero, it can be shown that equation (8) reduces to the dilute dispersion equation for spheres (eq. (2)). With this fact in mind the coating correction factor can be defined in the same manner that the shape factor was defined in the preceding section:

$$\text{Coating correction factor} = \frac{K_{(8)}}{K_{(2)}} \quad (9)$$

where the subscripts denote the values obtained by using equations (2) and (8).

The proposed model (eq. (7)) for anisotropic, coated particles then becomes:

$$K_{\text{eff}} = K_{(3)} \left[ \frac{K_{(4)}}{K_{(2)}} \right] \left[ \frac{K_{(8)}}{K_{(2)}} \right] \quad (10)$$

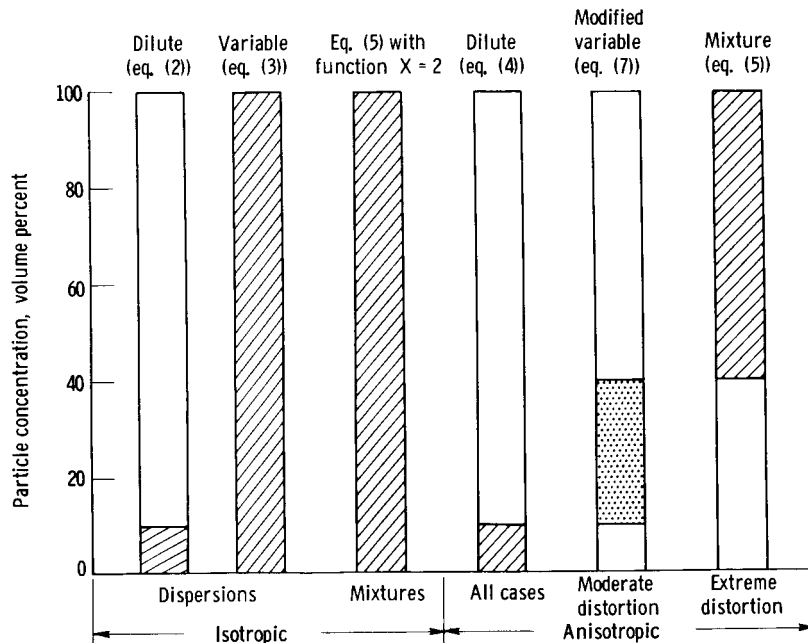


Figure 7. - Regions of applicability of equations for predicting thermal conductivity of tungsten - uranium dioxide dispersions.

which is the thermal conductivity of the variable dispersion equation (eq. (3)) multiplied by the appropriate shape and coating factors. An unusual application of the coating model will be presented in the section Additional Data.

## Regions of Applicability

To define exactly where each of the analytical models described in the preceding sections is applicable would be impossible because there are several areas where overlapping occurs. The bar graph shown in figure 7 summarizes the various regions of concern and lists the equation which applies to each. The suggested model (eq. (7)) covers the region not presently included by the other equations and is of particular importance to the work being done on W- $\text{UO}_2$  dispersions. Appendix C graphically summarizes the variation of the thermal conductivity of W- $\text{UO}_2$  dispersions obtained by using this model as a function of several parameters.

## COMPARISON WITH EXPERIMENTAL RESULTS

### Data Obtained in Tungsten - Water-Moderated Reactor Program

A recent series of experiments (ref. 3) was conducted to determine the value of the

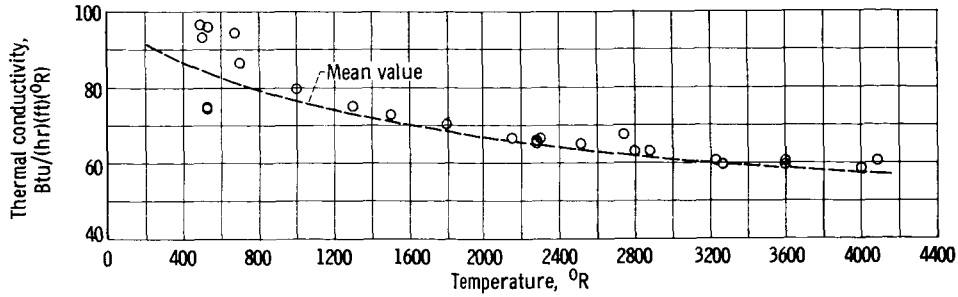


Figure 8. - Temperature variation of the thermal conductivity of tungsten. (Data taken from refs. 5 to 9.)

thermal conductivity of W-UO<sub>2</sub> dispersions with particle (UO<sub>2</sub>) concentrations up to 40 volume percent. The flash diffusivity method (appendix B), modified by the use of a laser beam instead of a xenon flash lamp (ref. 4), was used to determine the experimental values of the thermal conductivity.

To compare the results of this experimental study with the analytical model described in the section on analytical methods (p. 3), the conductivity of the two materials being used must be established (i. e., W and UO<sub>2</sub>).

Values for the thermal conductivity of tungsten can be found in references 5 to 9. The compilation of these data is shown in figure 8 and, except for the room temperature region, indicates good agreement among the various sources. The mean value curve superimposed on the data can be represented by

$$K_m = 98 - 27.48 \frac{T}{10^3} + 5.98 \left( \frac{T}{10^3} \right)^2 \quad \text{for } T < 1600^\circ \text{ R} \quad (11a)$$

$$K_m = 77.345 - \frac{T}{200} \quad \text{for } T \geq 1600^\circ \text{ R} \quad (11b)$$

Data on the conductivity of UO<sub>2</sub> from various sources has already been compiled by Cottrell (ref. 10) and Belle (ref. 11). The results are summarized by establishing the upper and lower limit lines shown in figure 9. The wide scatter can probably be attributed to the stoichiometric and density variations of the materials used by the different investigators.

The mean value curve for the conductivity of UO<sub>2</sub> can be expressed as follows:

$$K_p = 6.022 - 3.033 \frac{T}{10^3} + 0.4538 \left( \frac{T}{10^3} \right)^2 \quad \text{for } T \leq 3260^\circ \text{ R} \quad (12a)$$

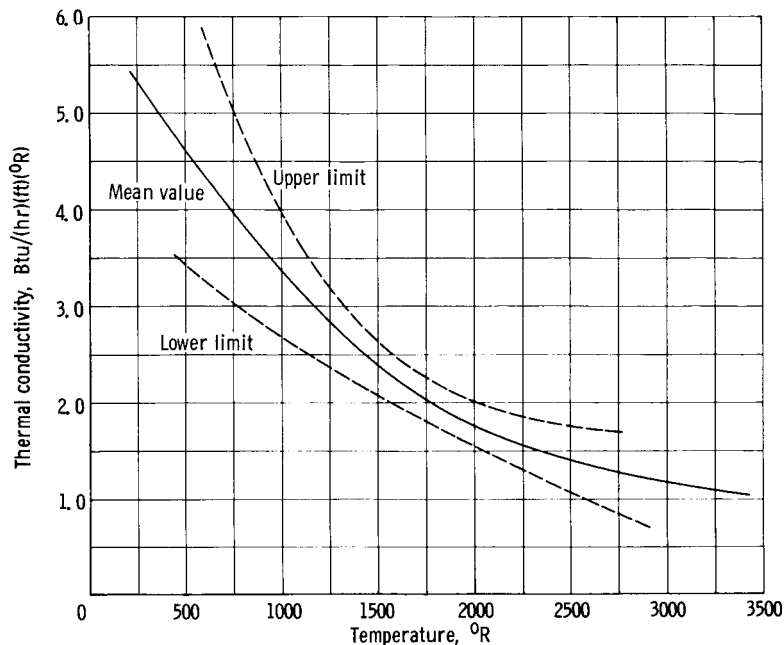


Figure 9. - Temperature variation of thermal conductivity of uranium dioxide. Limits based on data taken from references 10 and 11.

and

$$K_p = 1.0 \quad \text{for } T > 3260^\circ \text{ R} \quad (12b)$$

The mean values for the thermal conductivity of the base materials were used to investigate the effective conductivity of dispersions of  $\text{UO}_2$  particles in a tungsten matrix. The material used in the experiments (ref. 3) was manufactured by a rolling process; thus the particle shape is not strictly an oblate ellipsoid because the elongation in the direction of rolling is greater than that in the width direction. Visual examination of representative photomicrographs (fig. 5, p. 8) indicate (without an extensive statistical study) that the elongation is four to six times the particle thickness in the rolling direction and from two to three times the particle thickness in the direction perpendicular to the rolling direction. Because the analytical method of Fricke assumes that the two major axes are equal, the true solution to the anisotropic case for the above conditions is somewhere near the average, or a particle having an axis ratio (major to minor axis) of 3 or 4.

The results of the comparison shown in figure 10 indicate good agreement between the analytical and experimental values. In general, the scatter is compatible with the assumptions made in selecting the mean-value conductivity of W (fig. 8) and  $\text{UO}_2$  (fig. 9) if the potential errors in the experiments are considered. Parker (ref. 4) estimated that the flash diffusivity technique yielded results that were within  $\pm 10$  percent of previously established values. This agreement seems reasonable when the possible errors in the



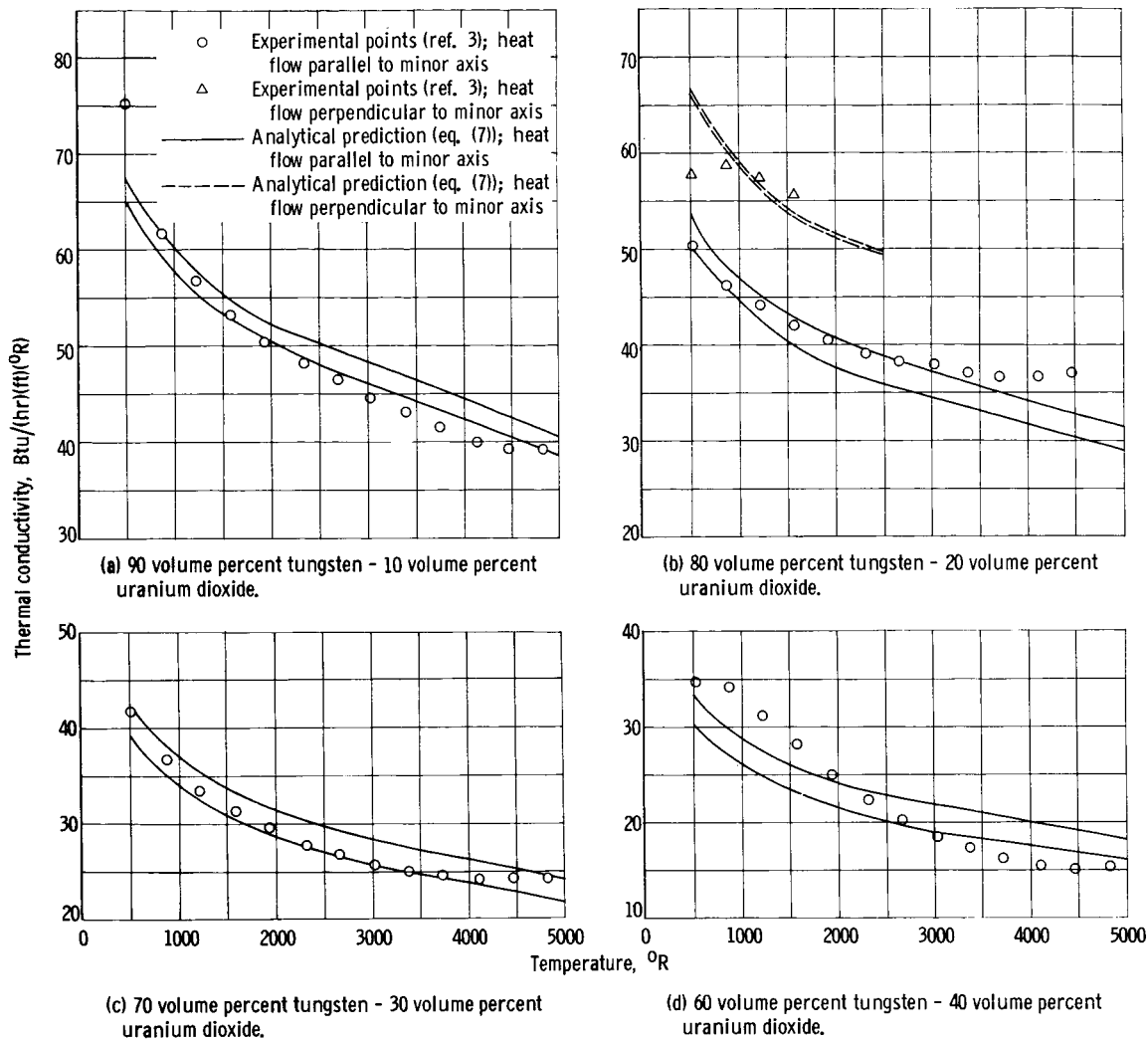


Figure 10. - Comparison of experimental and analytical values of thermal conductivity.

individual variables reported by Taylor (ref. 3), which were later used in the determination of the thermal conductivity, are considered:

|  |         |
|--|---------|
| Specific heat, $C_p$ , percent error . . . . .   | $\pm 4$ |
| Room temperature density, $\rho_0$ (deviation from theoretical), percent error . . . . . | $\pm 3$ |
| Product, percent error . . . . .   | $\pm 7$ |

A potential source of error in Taylor's work, which is negligible at low temperatures but increases with temperature, is the use of room temperature dimensions (or densities) in the calculation of the thermal diffusivity and thermal conductivity. For the samples tested, the linear expansion over the entire range of temperatures was about 2 percent (ref. 3). When this factor is neglected, as shown in appendix B, the predicted values are high by the same amount. Thus, the scatter in this range of experiments is

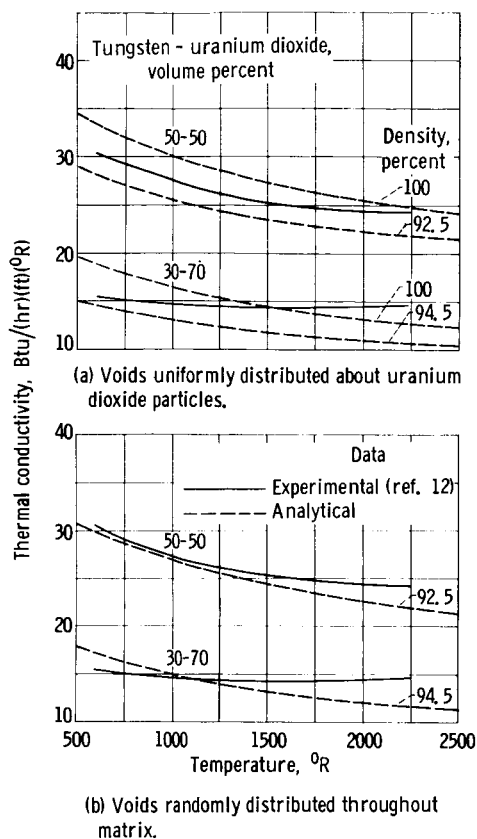


Figure 11. - Comparison of analytical and experimental results for tungsten - uranium dioxide dispersions.

at best between 7 and 9 percent with a tendency for the experimental values of thermal conductivity to be at the higher temperatures.

## Additional Data

Some additional experimental data for W- $\text{UO}_2$  dispersions is available for particle ( $\text{UO}_2$ ) concentrations of 50 and 70 volume percent and, although falling outside the range of interest for the tungsten-water-moderated reactor program (ref. 1), are compared to the analytical method described in the analytical methods section (p. 3).

These additional data (refs. 12 and 13) were obtained by using compacts rather than rolled plates; consequently, the shape factor of equation (7) reduces to 1.0 because the particles are probably not distorted. Applying the variable dispersion equation (eq. (3)) directly to the two cases results in the comparison shown in figure 11(a) as the 100-percent-dense line. The predicted values are generally higher than the experimental results, which can

probably be attributed to the fact that the 50- and 70-volume-percent- $\text{UO}_2$  samples were respectively only 92.5 and 94.5 percent dense at room temperature.


An attempt to include this parameter in the calculations can be made by the use of the previously discussed coating model (eq. (10)). If the voids are assumed to be uniformly distributed (i. e., each particle is surrounded by a void) and the fractional ratio of the two base materials is assumed to remain constant, an effective volume fraction of each species can be determined by multiplying the theoretical volume fraction by the density factor  $F_d$ . Thus, the effective volume fractions for the 50- and 70-volume-percent- $\text{UO}_2$  cases are as follows:

(1) 50 W-50  $\text{UO}_2$  volume percent

$$V'_m = V'_p = (0.925)(0.50) = 0.4625$$

$$\text{Void} = 1.0 - 0.925 = 0.075$$

(2) 30 W-70  $\text{UO}_2$  volume percent


$$V'_m = (0.945)(0.30) = 0.2835$$

$$V'_p = (0.945)(0.70) = 0.6615$$

$$\text{Void} = 1 - 0.945 = 0.055$$

Assuming that the conductivity of the void is negligible and substituting these values into equation (9) results in an effective coating correction factor that can then be applied to the 100-percent-dense values calculated in the preceding paragraphs. The results of this correction are also shown in figure 11 and do not seem to improve the error between the predicted and experimental values although the results of both calculations tend to bracket the experimental values and are generally within possible experimental error. There are several possible reasons, however, that might partially explain this discrepancy:


(1) The assumption that the voids are uniformly distributed about each particle may be in error.

(2) There is no assurance that the room-temperature, nontheoretical-density factor remains constant as the temperature is increased. For example, if a void did surround or contact a  $\text{UO}_2$  particle, the apparent density of the material (related to the theoretical value) might increase at the higher temperatures because of the greater expansion characteristics of the  $\text{UO}_2$  that would tend to displace the void. Of course, the reverse situation might occur if the void were isolated in the tungsten matrix.

An alternate method that accounts for the nontheoretical-density characteristics of the experiments (ref. 12) is to first calculate the thermal conductivity of the composite as though it were 100 percent dense. The resulting effective conductivity of the 100-percent-dense mixture is then used as the matrix conductivity, and the calculation is repeated with the particle concentration now corresponding to the measured void fraction of the W- $\text{UO}_2$  compacts with the conductivity of the void assumed to be negligible. Figure 11(b) shows the result of such a calculation and indicates much better agreement than that of the preceding calculation, which used uniformly distributed voids about each particle (fig. 11(a)). A possible explanation for the discrepancy that still exists at higher temperatures may still follow the reasoning of item 2.

## CONCLUDING REMARKS

There are at least three basic models (ref. 2) that appear to be satisfactory for determining the thermal conductivity of dispersions:

- (1) The dilute dispersion model (eq. (2))
  - (2) The variable dispersion model (eq. (3))
  - (3) The mixture model (eq. (5))
- 

~~CONFIDENTIAL~~

In addition, anisotropic versions of the dilute dispersion model (eq. (4)) and the mixture model (eq. (5)) are also available. However, because of the assumptions made in the derivation of all these models, the range of applicability of each is limited.

One region of particular interest in the study of W-UO<sub>2</sub> dispersions is not covered by any of these models. A suggested model for this undefined region is proposed by noting the similarity in the results obtained from the dilute dispersion (eq. (2)) and variable dispersion (eq. (3)). The resulting equation for the effective thermal conductivity of W-UO<sub>2</sub> dispersions is given by

$$K_{\text{eff}(\text{corrected})} = K_{(3)} \left[ \frac{K_{(4)}}{K_{(2)}} \right] \quad (7)$$

where the subscripts refer to values obtained from equations (2), (3), and (4). This method of correcting for anisotropic effects is semiempirical in nature, because there is no true mathematical basis for such a procedure.

The suggested method, compared with experimental data (ref. 3), yields values that are within the expected experimental error. Therefore, this method, subject to the following restrictions, is offered to determine the thermal conductivity of anisotropic dispersions:

1. The particle concentration is greater than 10 volume percent and less than 40 volume percent.
2. The thermal conductivity of the matrix is greater than that of the particle (i. e.,  $K_m/K_p > 1.0$ ).

Because the amount of experimental data currently available on W-UO<sub>2</sub> dispersions is quite limited, the suggested method should be compared to the results of future experiments to extend the range and/or remove the restrictions currently imposed.

With an argument similar to that used in formulating the anisotropic correction factor for the variable dispersion case (eq. (7)), a coating correction factor, applicable when the particles are coated with a third material (e. g., niobium), can be defined so that the thermal conductivity is given by

$$K_{\text{eff}} = K_{(3)} \left[ \frac{K_{(4)}}{K_{(2)}} \right] \left[ \frac{K_{(8)}}{K_{(2)}} \right] \quad (10)$$

where the subscripts refer to the values obtained from the respective equations. While this equation is not presently applicable to the tungsten - water-moderated concept, it is presented for possible future reference.

Lewis Research Center,  
National Aeronautics and Space Administration,  
Cleveland, Ohio, May 11, 1965.

## APPENDIX A

### EQUATIONS USED TO DETERMINE THERMAL CONDUCTIVITY OF ANISOTROPIC DISPERSIONS

The original work done by Fricke, a biophysicist working on the electrical behavior of blood, was based on the random orientation of a dilute dispersion of ellipsoids. Power (ref. 2) shows how this work can be extended to two-directional preferred orientation. The result of this analysis is shown in the following equations:

#### Equations Used to Determine the Effective Conductivity of Anisotropic Dispersions

Dilute dispersion model. -

$$\frac{K_{\text{eff}}}{K_m} = \frac{R(1 + XV_p) + X(1 - V_p)}{R(1 - V_p) + (X + V_p)} \quad (\text{A1})$$

(Note that this is an alternate form of equation (4).)

Mixture model. -

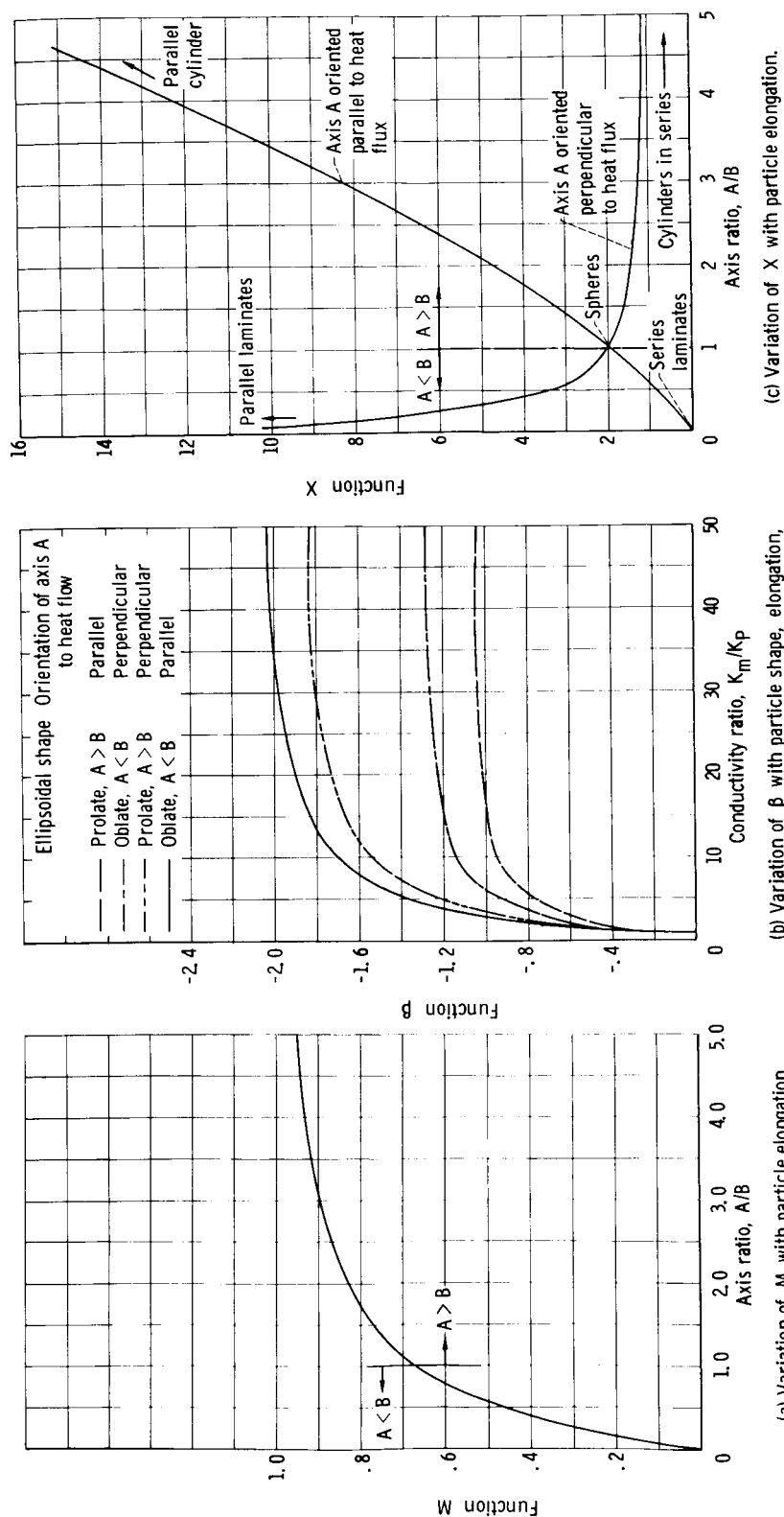
$$\frac{K_m - K_{\text{eff}}}{K_m + XK_{\text{eff}}} = \frac{V_p}{1 - V_p} \frac{K_{\text{eff}} - K_p}{K_p + XK_{\text{eff}}} \quad (\text{A2})$$

where

$$X = \frac{R(\beta - 1) + 1}{R - (\beta + 1)} \quad (\text{A3})$$

and

$$R = \frac{K_p}{K_m}$$

(a) Variation of  $M$  with particle elongation.(b) Variation of  $\beta$  with particle shape, elongation, and orientation; axis ratio, 5.(c) Variation of  $X$  with particle elongation.Figure 12 - Variations of functions  $M$ ,  $\beta$ , and  $X$  for several conditions.

Values of  $\beta$  for Various Conditions

For the A axis oriented parallel to the heat flux. -

$$\beta = \frac{R - 1}{1 + (R - 1)(1 - M)} \quad (A4)$$

For the A axis oriented perpendicular to the heat flux. -

$$\beta = \frac{R - 1}{1 + (R - 1) \frac{M}{2}} \quad (A5)$$

For random orientation. -

$$\beta = \frac{R - 1}{3} \left[ \frac{2}{1 + (R - 1) \frac{M}{2}} + \frac{1}{1 + (R - 1)(1 - M)} \right] \quad (A6)$$

where for  $A < B$

$$M = \left( \frac{\theta - \frac{1}{2} \sin 2\theta}{\sin^3 \theta} \right) \cos \theta \quad (A7)$$

$$\cos \theta = \frac{A}{B}$$

and for  $A > B$

$$M = \frac{1}{\sin^2 \varphi} - \frac{1}{2} \left( \frac{\cos^2 \varphi}{\sin^3 \varphi} \right) \log_e \left( \frac{1 + \sin \varphi}{1 - \sin \varphi} \right) \quad (A8)$$

$$\cos \varphi = \frac{B}{A}$$

The variation of  $M$ ,  $\beta$ , and  $X$  is shown in figure 12 for several conditions.

## APPENDIX B

### BRIEF DISCUSSION OF FLASH DIFFUSIVITY METHOD OF MEASURING THERMAL PROPERTIES OF SOLIDS

Included in this report is a comparison of the predicted values obtained with the suggested analytical model with experimental data (ref. 3) obtained by using a modified flash diffusivity method (ref. 4). To familiarize the reader with this method, a brief discussion of the procedures and pertinent equations used in the analysis is given.

In this method, a sample with initial thickness  $L_0$  and face area  $S_0$  is initially brought from ambient conditions  $T_0$  to an elevated temperature  $T_1$  by the use of auxiliary heaters (see fig. 13). From this new steady-state point, a small transient is induced by pulsing the front face of the specimen with a laser beam. From the characteristic temperature rise of the rear surface of the sample, the thermal diffusivity, the heat capacity, and finally the thermal conductivity of the material can be determined.

Parker, et al. (ref. 4), shows that the thermal diffusivity under these conditions can be expressed as

$$\alpha_T = \frac{1.38 L^2}{\pi^2 \tau} \quad (B1)$$

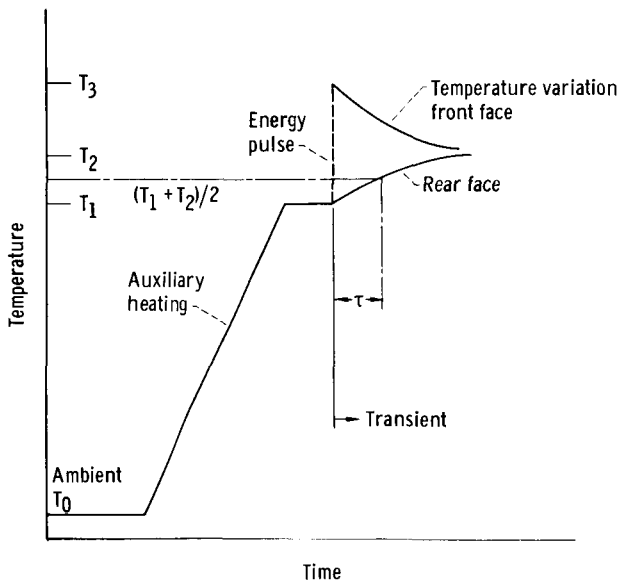


Figure 13. - Schematic time-temperature variation during flash diffusivity method of obtaining thermal conductivity.

where  $\tau$  is the time necessary for the rear surface to reach half the temperature rise from  $T_1$  to  $T_2$ . This method was used to predict the thermal diffusivity of Armco iron, which has fairly well-known thermal characteristics. The results (ref. 3) verify the validity of this procedure (eq. (B1)). Some question exists, however, as to the proper value of thickness that should be used if the expansion of the material is significant between the ambient and the testing temperature.

Parker shows that the effective temperature at which the above diffusivity is actually measured is equal to the steady-state value  $T_1$  plus a mean temperature rise that



can be approximated by

$$\Delta T = 1.6(T_2 - T_1) \quad (B2)$$

The factor 1.6 is greater than unity because the expression is a time-averaged value of the temperature rise for the entire sample. The front face of the sample has an initially larger value  $T_3$  relative to the rear face (fig. 7, p. 13).

For most of the experimental measurements (ref. 3), the transient temperature rise  $\Delta T$  was small compared to the absolute temperature level at the start of the transient. For all practical purposes, the effective temperature and the steady-state temperature  $T_1$  are nearly equal for this series of experiments.

From the basic definition of the thermal diffusivity, the thermal conductivity is given by

$$K_T = (\alpha \rho C_p)_T \quad (B3)$$

and, from the conservation of energy, a relation between the product of the density and specific heat and the energy emitted by the laser is obtained (ref. 4)

$$(\rho C_p)_T = \frac{E}{LS \Delta T} \quad (B4)$$

When the equations (B1) and (B4) are substituted into the basic definition (eq. (B3)), the required expression for the thermal conductivity is obtained

$$K_T = \left( \frac{1.38 E}{\pi^2 \tau \Delta T} \right) \left( \frac{L}{S} \right)_T \quad (B5a)$$

For materials with isotropic expansion characteristics, the change in length with temperature is related directly to the linear coefficient of expansion, while the change in area and volume are respectively related to the square and cube of the same constant. The ratio  $L/S$  evaluated at temperature  $T$  can thus be expressed as

$$\left( \frac{L}{S} \right)_T = \left[ \frac{L(1 + \epsilon)}{S(1 + \epsilon)^2} \right] = \frac{L_0}{S_0(1 + \epsilon)}$$

where  $\epsilon$  is the linear elongation between the ambient and the testing conditions.

Substituting this relation into equation (B5a) yields the following expression for ob-

[REDACTED]

taining the thermal conductivity by the flash diffusivity method

$$K_T = \left( \frac{1.38 E}{\pi^2 \tau \Delta T} \right) \left( \frac{L}{S} \right)_0 \left( \frac{1}{1 + \epsilon} \right) \quad (B5b)$$

In lieu of obtaining the specific heat from the conservation of energy (eq. (B4)), Taylor (ref. 3) used previously established values for the specific heat of the two components and then determined the properly weighted specific heat of the composite. The error associated with the variable  $C_p$  obtained in this manner was estimated (ref. 3) to be  $\pm 4$  percent. An alternate form of equation (B5b) can be obtained for this case. Combining equations (B1) and (B3) and noting that

$$\rho_T = \frac{\rho_0}{(1 + \epsilon)^3}$$

yield the following relation:

$$K_T = \frac{1.38 L_0^2 \rho_0 (C_p)_T}{\pi^2 \tau (1 + \epsilon)} \quad (B5c)$$

In essence, both forms of equation (B5) indicate that the thermal conductivity obtained by the flash diffusivity method should be corrected by the cube root of the density change to account for the expansion characteristics of the material. When the difference between the testing temperature and the ambient temperature is small, and/or the thermal coefficient of expansion is negligible, sufficient accuracy can be obtained by using the room temperature values of  $L$  and  $S$  and by neglecting the ratio involving the expansion term. This condition, however, is not always true, and the expansion factor may become significant when the testing temperatures are as high as they are in the W-UO<sub>2</sub> experiments.

## APPENDIX C

### VARIATION OF THERMAL CONDUCTIVITY OF TUNGSTEN - URANIUM DIOXIDE DISPERSIONS AS FUNCTION OF SEVERAL PARAMETERS

Figures 14 to 18 show a summary of the thermal conductivity behavior of W-UO<sub>2</sub> dispersions. These values were calculated by using the suggested method described in the text (eq. (7)) and by utilizing the mean value thermal conductivities of the two base materials (figs. 8, p. 13 and 9, p. 14). Except for figure 18, all of the cases were calculated by using oblate ellipsoids where axis  $A < B = C$ .

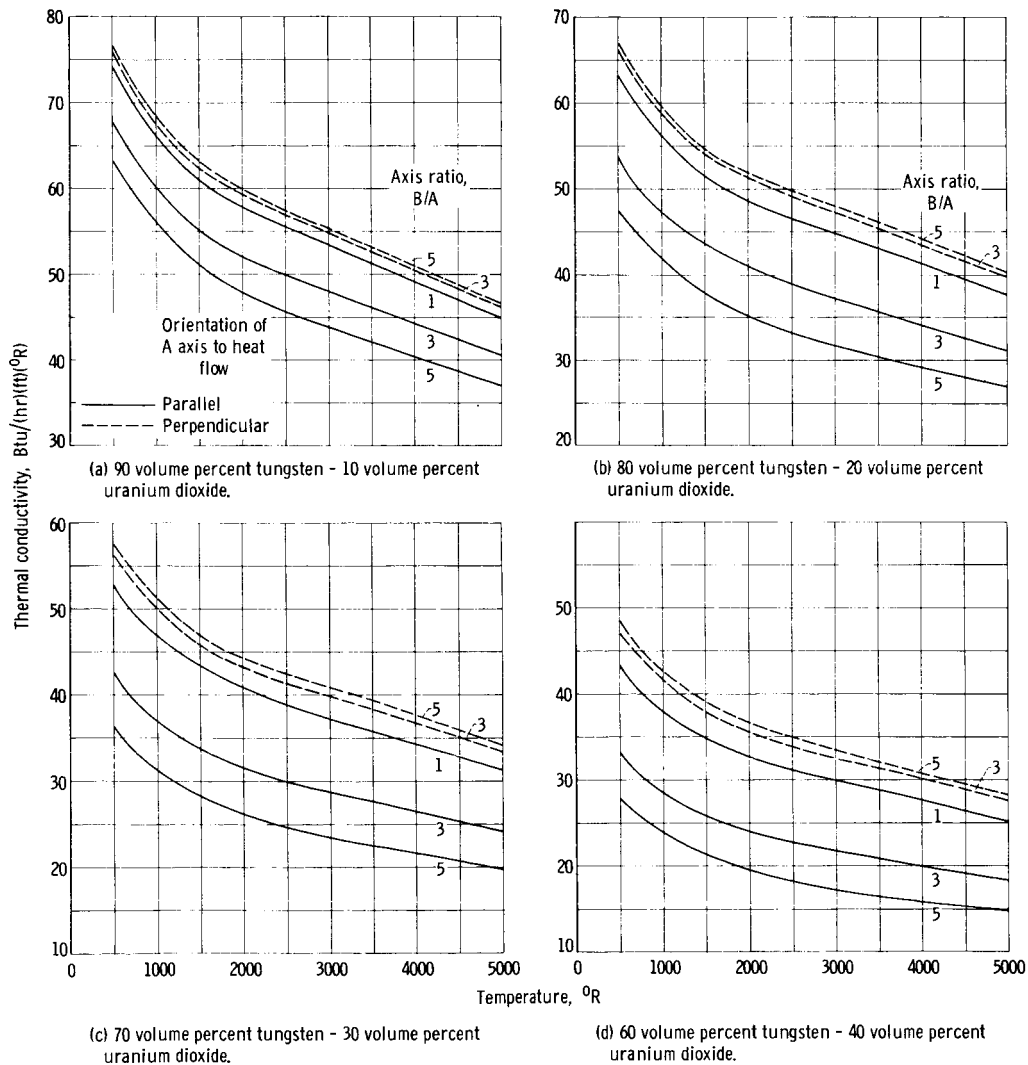


Figure 14. - Effect of particle elongation on thermal conductivity of tungsten - uranium dioxide dispersions.

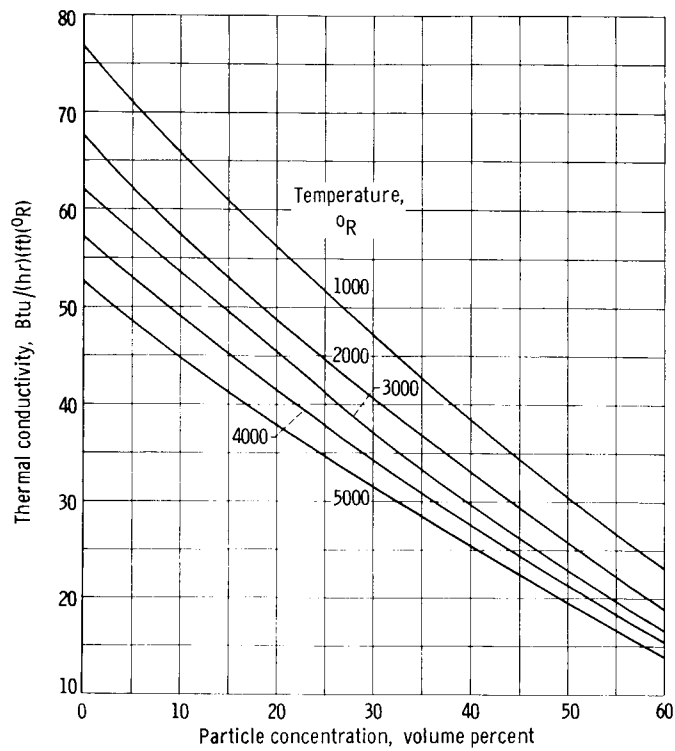


Figure 15. - Effect of temperature on the thermal conductivity of tungsten - uranium dioxide dispersions for spherical particles.

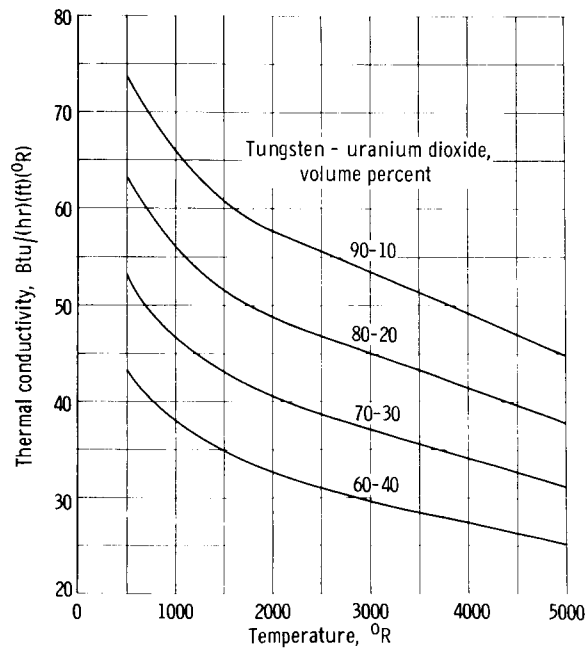


Figure 16. - Effect of particle concentration on thermal conductivity of tungsten - uranium dioxide dispersions for spherical particles.

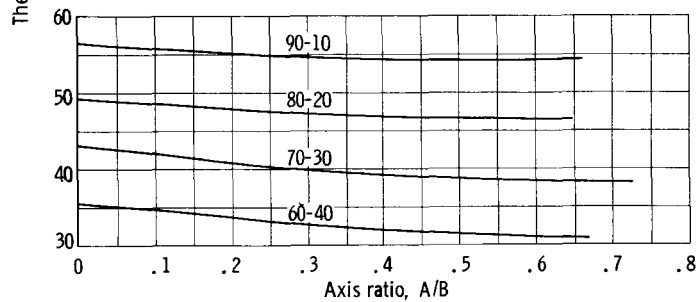
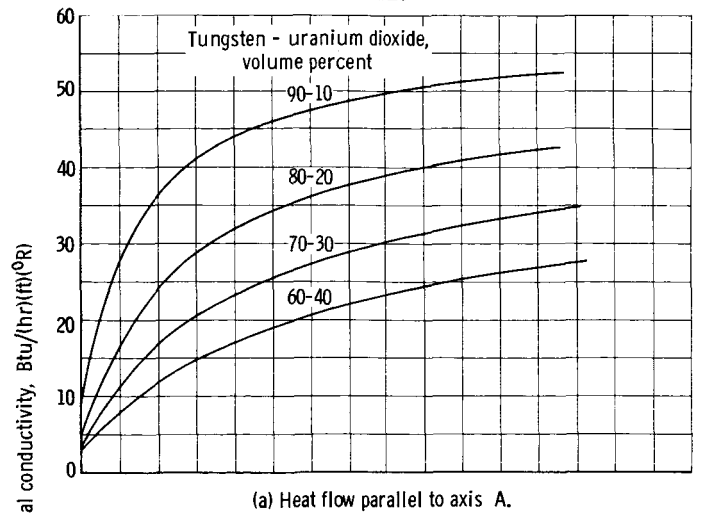


Figure 17. - Effect of axis ratio on thermal conductivity of tungsten - uranium dioxide dispersions; temperature, 3000° R.

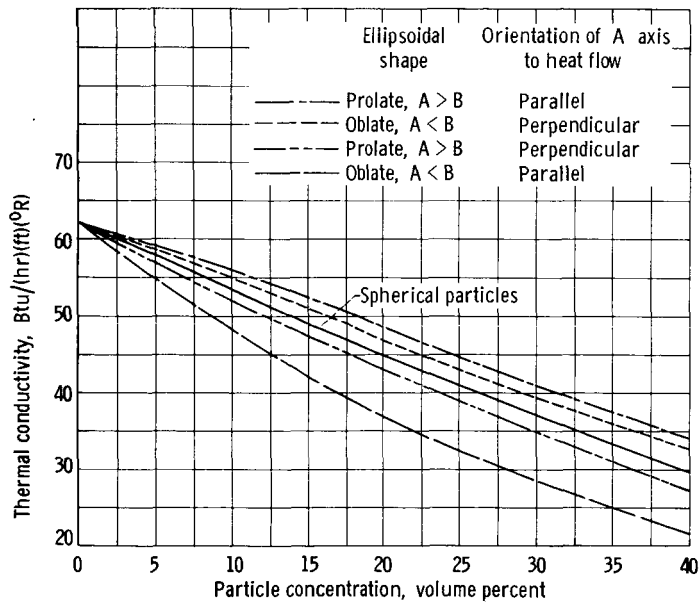


Figure 18. - Effect of particle shape and orientation on thermal conductivity of tungsten - uranium dioxide dispersions; temperature, 3000° R; axis ratio, 3.

## APPENDIX D

### SYMBOLS

|            |   |             |                                   |
|------------|---|-------------|-----------------------------------|
| A, B, C    | axis of ellipsoid, ft                                       | $\beta$     | function defined by equation (6)  |
| $C_p$      | specific heat at constant pressure, Btu/(lb)( $^{\circ}$ R) | $\gamma$    | ratio of mean field strengths     |
| E          | energy emitted by laser, Btu                                | $\epsilon$  | elongation, ft/ft                 |
| $F_d$      | fraction of theoretical density                             | $\theta$    | angle defined in appendix A       |
| K          | thermal conductivity, Btu/(hr)(ft)( $^{\circ}$ R)           | $\rho$      | density, lb/cu ft                 |
| L          | thickness of sample, ft                                     | $\tau$      | time increment, hr                |
| M          | function defined in appendix A                              | $\varphi$   | angle defined in appendix A       |
| Q          | heat generation rate, Btu/(hr)(cu ft)                       | Subscripts: |                                   |
| R          | ratios of thermal conductivities, $K_p/K_m$                 | c           | condition in the coating          |
| S          | face area of sample, sq ft                                  | eff         | effective value of the mixture    |
| T          | temperature, $^{\circ}$ R                                   | m           | condition in the matrix           |
| $\Delta T$ | temperature difference, $^{\circ}$ R                        | max         | refers to maximum value           |
| V          | volume fraction   | p           | condition in the particle         |
| X          | function defined by equation (6)                            | T           | evaluated at temperature T        |
| $\alpha$   | thermal diffusivity, sq ft/hr                               | w           | condition at the wall             |
|            |   | 0           | refers to initial conditions      |
|            |   | 1           | refers to conditions at point (1) |
|            |   | 2           | refers to conditions at point (2) |

## REFERENCES

1. Rom, Frank E.; and Ragsdale, Robert G.: Advanced Concepts for Nuclear Rocket Propulsion. Proceedings of the NASA-University Conference on the Science and Technology of Space Exploration, NASA SP-20, 1962, pp. 3-15.
2. Powers, A. E.: Conductivity in Aggregates. Rept. No. KAPL-2145, Knolls Atomic Power Lab., General Electric Co., Mar. 6, 1961.
3. Taylor, R. E.: Thermal Properties of Tungsten-Uranium Dioxide Mixtures. NASA CR-54141, 1964.
4. Parker, W. J.; Jenkins, R. J.; Butler, C. P.; and Abbott, G. L.: Flash Method of Determining Thermal Diffusivity, Heat Capacity, and Thermal Conductivity. J. Appl. Phys., vol. 32, no. 9, Sept. 1961, pp. 1679-1684.
5. Anon.: Tungsten. Metallwerk Plansee (Austria), 1963.
6. Schmidt, F. F.; and Ogden, H. R.: The Engineering Properties of Tungsten and Tungsten Alloys. Rept. No. DMIC-191, Battelle Memorial Inst., Sept. 27, 1963.
7. Anon.: How Tungsten Does it Better. Bull. No. MI-5301, Fansteel Metallurgical Corp., 1963.
8. Hogerton, J. F.; and Grass, R. C., eds.: General Properties of Materials, The Reactor Handbook. Vol. 3 - Materials. Sec. 1 - General Properties. AECD-3647, AEC, Mar. 1955.
9. Goldsmith, Alexander; Waterman, Thomas E.; and Hirschhorn, Harry J.: Thermo-physical Properties of Solid Materials. Vol. 1 - Elements. Rept. No. TR-476, WADD, Aug. 1960.
10. Cottrell, W. B.; Culver, H. N.; Scott, J. L.; and Yarosh, M. M.: Fission-Product Release From  $\text{UO}_2$ . ORNL-2935, Oak Ridge Nat. Lab., Sept. 13, 1960.
11. Belle, Jack, ed.: Uranium Dioxide: Properties and Nuclear Applications. AEC, 1961.
12. Dayton, Russell W.; and Dickerson, Ronald F.: Progress Relating to Civilian Applications During February 1963. Rept. No. BMI-1619, Battelle Memorial Inst., Mar. 1, 1963.
13. Dayton, Russell W.; and Dickerson, Ronald F.: Progress Relating to Civilian Applications During April 1963. Rept. No. BMI-1630, Battelle Memorial Inst., May 1, 1963.